Alveolar epithelial surface area-volume relationship in isolated rat lungs

DANIEL J. TSCHUMPERLIN AND SUSAN S. MARGULIES
Department of Bioengineering, University of Pennsylvania, Philadelphia, Pennsylvania 19104

Tschumperlin, Daniel J., and Susan S. Margulies. Alveolar epithelial surface area-volume relationship in isolated rat lungs. *J. Appl. Physiol.* 86(6): 2026–2033, 1999.—In vitro studies of the alveolar epithelial response to deformation require knowledge of the in situ mechanical environment of these cells. Because of the presence of tissue folding and crumpling, previous measurements of the alveolar surface area available for gas exchange are not equivalent to the epithelial surface area. To identify epithelial deformations in uniformly inflated lungs representative of the in vivo condition, we studied isolated Sprague-Dawley rat lungs ($n = 31$) fixed by perfusion with glutaraldehyde on deflation after cycling three times at high lung volume (10–25 cmH_2O). The epithelial basement membrane in 45 electron micrographs (×12,000)/rat was traced, digitally scanned, and analyzed. Epithelial basement membrane surface area (EBMSA) was computed from a morphometric relationship. EBMSA was found to increase 5, 16, 12, and 40% relative to EBMSA at 24% total lung capacity at lung volumes of 42, 60, 82, and 100% total lung capacity, respectively. The increases in EBMSA suggest that epithelial cells undergo significant deformations with large inflations and that alveolar basement membrane deformation may contribute to lung recoil at high lung pressures.

lung mechanics; lung anatomy; cell strain; pulmonary; respiratory

PREVIOUS INVESTIGATIONS have demonstrated a variety of deformation-induced responses of the intact lung (3, 7, 10, 17, 29). Alveolar epithelial cells, which line the gas-exchange surface of the lung, are believed to play an important role in the transduction of physical stimuli associated with inflation. Specifically, in vitro investigations have demonstrated that mature and fetal alveolar epithelial cells respond to deformation with increased cellular proliferation (9, 19), prostacyclin production (20), surfactant secretion (28), and surfactant-related phospholipid synthesis (19). These studies established the importance of the biomechanical environment in modulating alveolar epithelial physiology. However, little is known about the relationship between local cellular deformations and overall changes in lung volume. This relationship must be identified to relate changes in cellular function during in vitro deformation to those that would be expected for respiratory maneuvers such as spontaneous breathing, yawning, fetal breathing movements, and mechanical ventilation.

Studies incorporating morphometric stereology with light and electron microscopy have been instrumental in identifying changes in lung microstructure with inflation and deflation (2, 5, 6, 13). Using light microscopy (×400), Gil et al. (5) observed that pleating of the alveolar surface varied with lung fixation volume. Consequently, estimates of alveolar surface area (surface available for gas exchange), such as those obtained by Gil et al. and Mercer et al. (13), are not analogous to estimates of epithelial surface area. Later, Bachofen et al. (2) examined lungs fixed on inflation from collapse, deflation, and reinflation by using electron microscopy (×10,000) to study the changes in both the alveolar surface area and the alveolar epithelial basement membrane surface area (EBMSA) with lung volume. They found that the degree of unfolding and stretching of the epithelium depended strongly on the lung volume history before fixation. More recently, Oldmixon and Hoppin (15) confirmed that alveolar septal folding is heavily dependent on the volume history of fixed lungs and suggested that septal folds form at low transpulmonary pressure (Ptp; <3 cmH_2O) during experimental procedures and may not be present in vivo. Because the focus of the study by Bachofen et al. was on the first inflation-deflation cycle of collapsed lungs (Ptp <1 cmH_2O), it is difficult to extrapolate their data to estimate an in vivo relationship between alveolar epithelial surface area and lung volume.

Therefore, the purpose of this study was to define the quasi-static relationship between EBMSA and Ptp, and EBMSA and volume by using isolated rat lungs fixed on deflation from total lung capacity (TLC) after cycling the lungs three times between TLC and 8–10 cmH_2O. Our results indicate that changes in EBMSA are relatively small at low lung volumes, but, at higher lung volumes, lung inflation is accompanied by stretching of septal tissue, resulting in large changes (~40%) in the alveolar EBMSA near the limits of inflation.

METHODS

Lung preparation. The experimental protocol was approved by the University of Pennsylvania Institutional Animal Care and Use Committee. Thirty-one female Sprague-Dawley rats (175–225 g, Charles River) were anesthetized with pentobarbital sodium (50 mg/kg, Nembutal, Abbott) and heparinized (2,000 U/kg). After tracheotomy, a size-18 cannula was inserted in the trachea, and rats were ventilated with room air at 60 breaths/min, 3-ml tidal volume, and 4 cmH_2O positive end-expiratory pressure. The chest was opened, and the inspiratory capacity (IC) of each rat, defined as the lung volume between 4 [functional residual capacity (FRC)] and 25 cmH_2O (TLC), was obtained by using a calibrated glass syringe and pressure transducer (P23ID, Gould). For lungs to be fixed at volumes other than TLC or FRC, the pressure corresponding to the volume of interest

The costs of publication of this article were defrayed in part by the payment of page charges. The article must therefore be hereby marked "*advertisement*" in accordance with 18 U.S.C. Section 1734 solely to indicate this fact.

was identified. Volumes studied included TLC, FRC, and FRC + 1/3 IC, + 2/3 IC, and −1/3 IC. The pulmonary artery was cannulated, and the left atrium and ventricle were punctured to allow passive release of perfusate. Lungs were perfused with 3% dextran T70 in a buffered salt solution (pH 7.4, 280 mosM) until all blood was cleared.

Lung isolation and fixation. Lungs were excised and suspended from a force transducer to detect and eliminate edematous lungs. Ptp was maintained by venting a constant-flow air source through an adjustable column of water. After cycling three times between TLC and 8–10 cmH_2O to provide a uniform inflation history and minimize septal pleating, lungs were deflated to the pressure corresponding to the lung volume of interest. Perfusion fixation with 2.5% glutaraldehyde (pH 7.4, 500 mosM, with 3% dextran T70, in 0.15 M cacodylate buffer) was begun, with arterial pressure (Ppa) maintained ~12 mmHg above alveolar pressure (PA) with a peristaltic pump to produce zone 2 conditions in the lung. After 30 min, perfusion of fixative was discontinued and the volume of the excised tissue (heart, lungs, trachea) was determined by volumetry (18). After the trachea and heart were separated from the lungs, the combined tracheal and heart volume was obtained, and the total lung volume (Vtot) was measured by subtracting the volume of the heart and trachea from the volume of the excised tissue. Air volume (Vair) of the lungs was computed by subtracting the tissue volume (Vti), which was computed from the weight of the lungs, assuming a density of 1 g/ml (Vair = Vtot − Vti).

Tissue sampling. The left lung of each animal was cut into equal thirds and fixed overnight in glutaraldehyde. A thin transverse section of each one-third was cut, and 10 blocks (~3 × 1 × 1 mm) were obtained from each section in the dorsal area of the lung, posterior to the major bronchi and blood vessels. Tissue blocks were refrigerated in 0.15 M cacodylate (pH 7.4, 290 mosM). Seven blocks from each third were selected randomly and processed for electron microscopy. Processing included postfixation with 1% OsO_4, 0.8% FeCN, and 1% uranyl acetate and ended with tissue embedded in Epon. Two transverse slices from each region of four lungs at TLC and FRC were embedded in paraffin for light microscopic determination of the volume fraction of large airways and vessels.

Electron microscopy. Thin slices (1 μm) of the Epon-embedded tissue were cut and stained with toluidine blue for light microscopy. After a two-level sampling approach (24), tissue was examined at the light microscopy level to prevent morphometric sampling of large airways and vessels. The computation of EBMSA took this into account by multiplying surface density by the parenchymal lung volume, which excludes the volume of large airways and vessels (see *Eq. 2*). One ultrathin section (70 nm) from each third of each lung was mounted on a 400-mesh copper grid and examined in the electron microscope. Micrographs were obtained by using the systemic quadrant method, where the field location to be photographed was fixed within the grid square (2). The first field was randomly selected, and subsequent fields were systematically evaluated in every other grid square in every other row. The evaluation of every second grid square in every second row was used to ensure a distribution of micrographs over the sample. If no tissue was present in a field, no picture was taken, but the number of empty fields (air space) was recorded. This information was used in the surface density calculation (see *Eq. 1*), where the summed length of contour lines was divided by the total area examined, including blank fields that were not photographed. A total of 15 fields from each sample that contained tissue was photographed at ×4,000 magnification. Negatives were photographically enlarged and printed at a final magnification of ×12,000, for an approximate field size of 330 μm^2. A total of 45 pictures from each animal was printed, 15 each from the upper, middle, and lower third of each lung.

Data analysis. The epithelial basement membrane in each print was traced on transparency film, digitally scanned, and analyzed to obtain epithelial contour length (NIH Image). Contour length data from all the micrographs were entered in a database and summed for each animal. The total length L (sum of contours) was divided by the total area analyzed A (printed and empty fields). This length per unit area was transformed into surface density (S/V), using the morphometric relationship (25)

$$S/V = \frac{\pi}{4} * \frac{L}{A} \quad (1)$$

The total EBMSA was calculated by multiplying S/V by the parenchymal lung volume. Parenchymal volume was defined as the total lung volume (Vtot) minus the volume composed of large airways and vessels. The volume fraction of large airways and vessels (X_{np}) at FRC and TLC was determined by point counting of the paraffin-embedded sections by using light microscopy (×100 magnification). Parenchymal volume was normalized across animals by TLC. The overall relationship between EBMSA and surface density is

$$\text{EBMSA} = V_{tot}(1 - X_{np})\left(\frac{TLC_{avg}}{TLC}\right)(S/V) \quad (2)$$

where TLC_{avg} is TLC across animals average.

RESULTS

The physiological and morphometric results for each lung volume studied are summarized in Tables 1 and 2, respectively. In general, the fixed lungs exhibited the expected nonlinear pressure (Ptp)-volume (Vair) relationship (Fig. 1) and confirmed that lungs were studied over their entire vital capacity. The measured IC and TLC are in close agreement with previous measurements in rats (13, 22).

Table 1. *Physiological measurements*

%TLC	*n*	Body Wt, g	Ptp, cmH_2O	Pa, cmH_2O	Vtot, ml	Vair, ml	IC, ml	TLC, ml
100 ± 0	7	203 ± 5	25.0 ± 0.0	37.2 ± 1.0	12.9 ± 0.9	11.5 ± 0.8	7.0 ± 0.3	11.5 ± 0.8
82 ± 0	6	207 ± 3	8.8 ± 0.4	21.2 ± 1.3	11.3 ± 0.3	10.0 ± 0.3	6.6 ± 0.2	12.2 ± 0.3
60 ± 2	6	200 ± 7	5.5 ± 0.4	16.5 ± 1.6	8.2 ± 0.8	7.0 ± 0.8	6.7 ± 0.4	11.4 ± 1.0
42 ± 2	6	206 ± 8	3.8 ± 0.2	15.7 ± 1.1	6.3 ± 0.6	5.2 ± 0.6	6.9 ± 0.3	12.2 ± 0.8
24 ± 2	6	206 ± 7	2.0 ± 0.2	14.3 ± 1.1	4.0 ± 0.5	3.0 ± 0.5	6.8 ± 0.4	12.0 ± 0.9

Values are means ± SE. *n*, No. of lungs; TLC, total lung capacity; Ptp, transpulmonary pressure; Pa, perfusion pressure at the pulmonary artery; Vtot, total lung volume; Vair, lung air volume; IC, inspiratory capacity.

Table 2. *Morphometric measurements*

%TLC	*S*/V, cm^{-1}	EBMSA, cm^2	$\%\Delta EBMSA_{24}$	$\%\Delta EBMSA_{42}$	$1 - X_{np}$
100 ± 0	262 ± 23	3,107 ± 289	40	34	0.87 ± 0.008
82 ± 0	256 ± 16	2,499 ± 159	12	8	
60 ± 2	341 ± 23	2,578 ± 169	16	11	
42 ± 2	432 ± 36	2,325 ± 139	5	0	0.87 ± 0.004
24 ± 2	649 ± 49	2,222 ± 110	0		

Values are means ± SE. *S*/V, epithelial basement membrane surface-to-volume ratio; EBMSA, epithelial basement membrane surface area; $\%\Delta EBMSA_{24}$ and $\%\Delta EBMSA_{42}$, percent increase in EBMSA relative to EMBSA measured at lung volumes of 24 and 42% TLC, respectively; X_{np}, volume fraction of nonparenchymal tissue.

Tissue examined at the light microscopy level (Fig. 2) appeared nearly identical to that described previously (5), with bulging capillaries and surface irregularities at low volumes, gradually changing to smooth surfaces and thin, flattened capillaries at elevated lung volumes.

Previous studies have estimated X_{np} by using a variety of methods, ranging from assuming that the airways and vessels compose a static volume (hence an increasing volume fraction of the lung on deflation) (6) to assuming the airways and vessels compose a nearly constant fraction of the lung, changing dimensions in harmony with the surrounding lung tissue (5). We carried out a limited investigation of this issue by examining six hematoxylin- and eosin-stained transverse lung sections from each of four lungs at 42 and 100% TLC. We found that X_{np} was indistinguishable (Student's *t*-test) between 42 and 100% TLC (Table 2). Gil et al. (5) examined lung tissue fixed at four volumes between 40 and 100% TLC, estimating the parenchymal volume by using air volume measured with a spirometer and air space fraction found by point counting in the sampled tissue. For comparison with the present study, we computed the volume fraction of parenchyma ($X_p = 1 - X_{np}$) from their data by dividing estimated parenchymal volume by measured organ volume, which yields X_p in the range of 0.86–0.89, with no clear relationship to lung volume. This range is comparable to our finding of X_p equal to 0.87, which we subsequently used as the parenchymal volume fraction at each lung volume (*Eq. 2*).

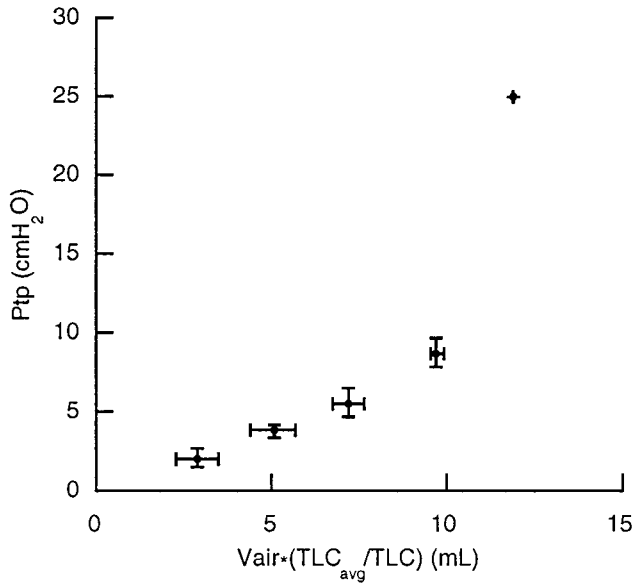

Fig. 1. Pressure-volume relationship for fixed lungs. Values are means ± SE. See Table 1 for *n* in each group. Pressure was determined with a transducer before fixation. Air volume was determined at conclusion of fixation by method of Scherle (18) and was normalized by average total lung capacity (TLC_{avg}) across animals. Ptp, transpulmonary pressure; Vair, air volume of lung.

EBMSA was calculated by using *Eq. 2*. No regional differences were found when results for the upper, middle, and lower one-third of lungs were compared, so data from 45 prints were summed for each animal to compute surface density. A regression curve fit to the means of the EBMSA and lung volume data shows that this relationship was well represented ($r^2 = 0.85$) by a second-order polynomial (Fig. 3*A*). EBMSA decreased most rapidly at high lung volumes. This trait is similar to the rapid drop in pressure from TLC to 82% TLC, so that a linear regression fit to the mean EBMSA and Ptp data (Fig. 3*B*) provides excellent agreement ($r^2 = 0.93$). Below 82% TLC, EBMSA is relatively constant, suggesting that further reductions in air volume occur primarily by crumpling of septal tissue, or reductions in alveolar duct volume. Overall, EBMSA is found to vary significantly with both lung volume (%TLC, $P < 0.005$) and Ptp ($P < 0.005$), when examined by one-way ANOVA by using the statistical package JMP (SAS Institute). Only lung volumes of 24 and 100% TLC differed significantly ($P < 0.05$), using the Tukey-Kramer honestly significant difference test for multiple comparisons. The variability in EBMSA data is probably due to both biological and technical variability inherent in animal studies and the limited number of randomly sampled micrographs examined, which represent only a small fraction of the overall lung volume.

DISCUSSION

Meaningful studies on the response of the alveolar epithelium to deformation require a knowledge of the mechanical environment of the cells in situ. The alveolar surface of the lung may increase by balloon-like stretching, accompanied by epithelial deformation, paper bag-like unfolding with no cellular deformation, or a combination of both mechanisms (2). Although changes in alveolar surface area with lung volume are relatively well studied (2, 5, 6, 13), cellular deformations with inflation are unknown. The lack of a definitive understanding of the importance of stretching and unfolding in lung volume changes prevents calculation of cellular deformations from previous measurements of changes in alveolar surface area and creates the need for a direct measurement of changes in epithelial surface area with lung volume.

The presently accepted method for examining changes in lung microstructure is morphometry of chemically fixed tissue at either the light- or electron-microscopic level. Although this method provides only an average epithelial deformation, it is the only imaging method

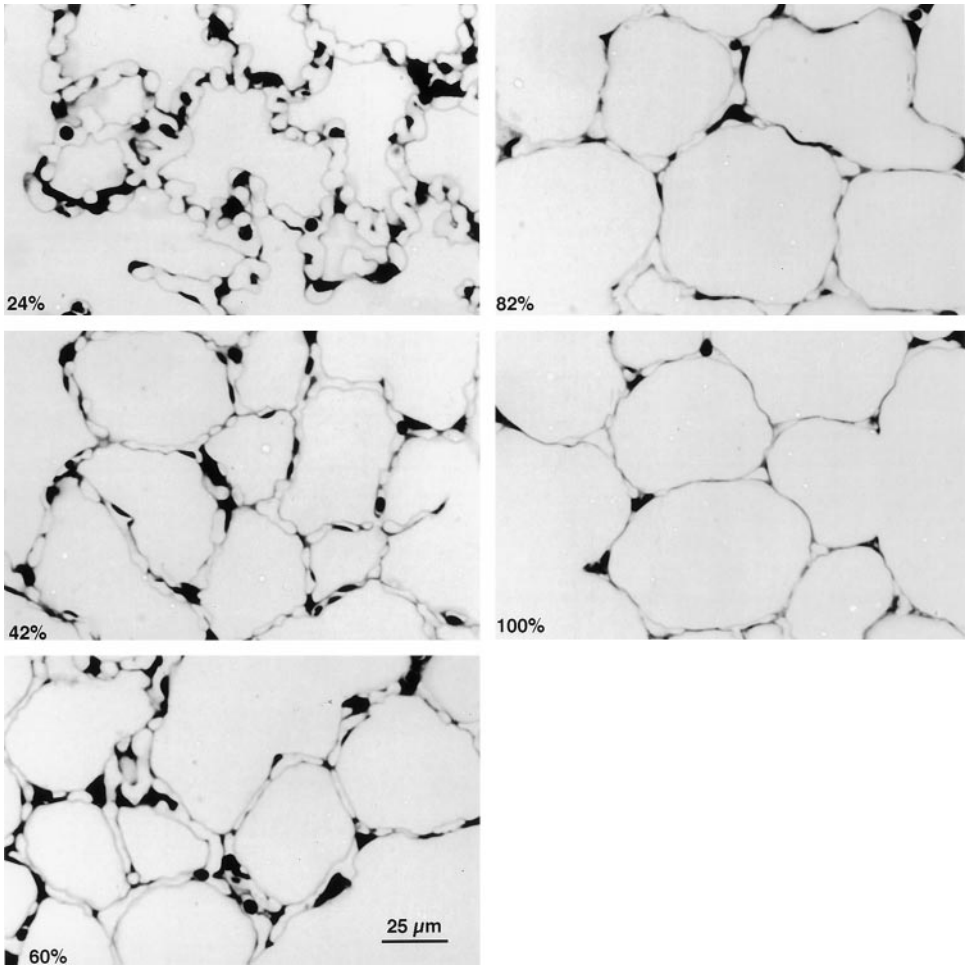

Fig. 2. Light micrographs of rat lungs fixed at each lung volume [%total lung capacity (TLC)] studied.

with sufficient resolution to study changes in surface area at the cellular level.

We therefore measured EBMSA in electron micrographs from isolated rat lungs fixed over a range of lung volumes. Our findings support the general hypothesis that, at low lung volumes, inflation of the lung can be accomplished without large changes in EBMSA, due to either unfolding of the alveolar epithelial surface or expansion of the alveolar ducts in the absence of alveolar inflation (Fig. 4). At high lung volumes, our findings indicate that significant changes in EBMSA occur, suggesting that the epithelial basement membrane and attached cells deform as the lung approaches physiological limits.

Changes in epithelial surface area with lung volume have been measured only once previously, by Bachofen et al. (2). Their fixation protocol differs from that in the present study in two critical respects. First, because of the toxicity of OsO_4, we chose to fix lungs by vascular perfusion with glutaraldehyde, then postfix with OsO_4 after cutting tissue into small blocks for embedding. Although this method provides optimal tissue preservation (1), the potential hazards associated with its use include retraction of fixed lungs on removal of inflation pressure and parenchymal distortion during tissue preparation. In a previous investigation using an identical fixation protocol, partial lung collapse was encountered on release of Ptp in rabbit lungs (1). To evaluate loss of lung volume at the termination of fixation, we glued two small paper markers to the pleural surface of three isolated lungs (~2–3 cm separating markers) during perfusion fixation at TLC. Care was taken to position the markers along a relatively planar portion of the lung surface. The linear distance between markers was measured with precision calipers (0.05-mm resolution) after 30 min of fixation just before and immediately after removal of the lungs from the constant-pressure source. No discernible change in marker separation was found in two of the experiments (<0.05 mm), and only a 2% change in linear dimension was found in a third, which is equivalent to an ~8% volume change. In general, we did not observe any collapse in rat lungs when inflation pressure was removed after 30 min of fixation, except for occasional regional collapse due to nonuniform perfusion, which resulted in the lungs being discarded without further study. The more complete fixation of rat lungs in this communication, compared with previous fixation of rabbit lungs (1) by using an identical fixation protocol, may be due to the smaller size of rat lungs (TLC ~12 ml in the rat vs. ~120 ml in the rabbit), which would allow for more uniform perfusion distribution throughout the lung, and therefore more uniform and complete fixation, or alternatively, may be due to species differences in the

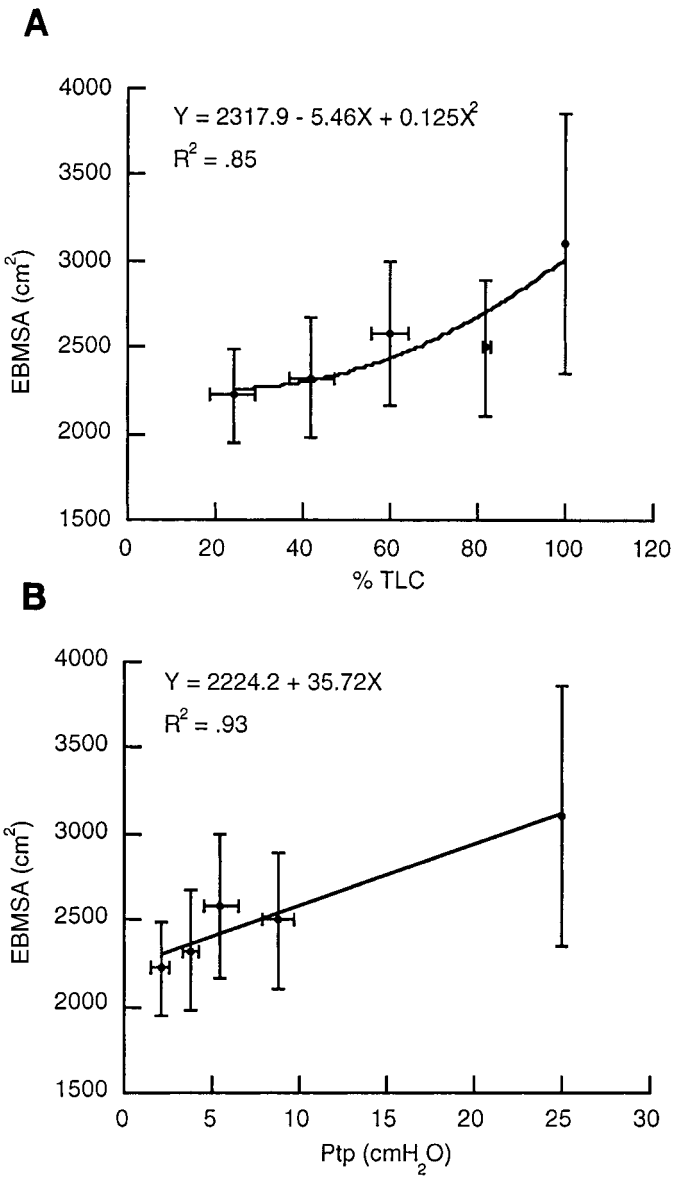

Fig. 3. Relationship between epithelial basement membrane surface area (EBMSA) and lung volume (*A*) and transpulmonary pressure (*B*), with best fit of means for each. Values are means ± SE. EBMSA was computed according to *Eq. 2*, with surface area normalized by TLC.

extracellular matrix, as discussed in detail below (12, 16).

Although there was little or no lung retraction on release of inflation pressure, it is possible that incomplete fixation could result in parenchymal distortions during tissue preparation. On cutting of the lungs, tissue was characterized as spongy, compressible, and able to deform, but it appeared to recover its original shape when unloaded and immersed in buffer. This has been described previously by Weibel (24) for glutaraldehyde-fixed lungs.

Because of the use of osmium as a postfixative, our protocol did not allow for in situ stiffening of elastin by ethanol dehydration. If not dehydrated, elastin can contract on the release of tension during tissue cutting

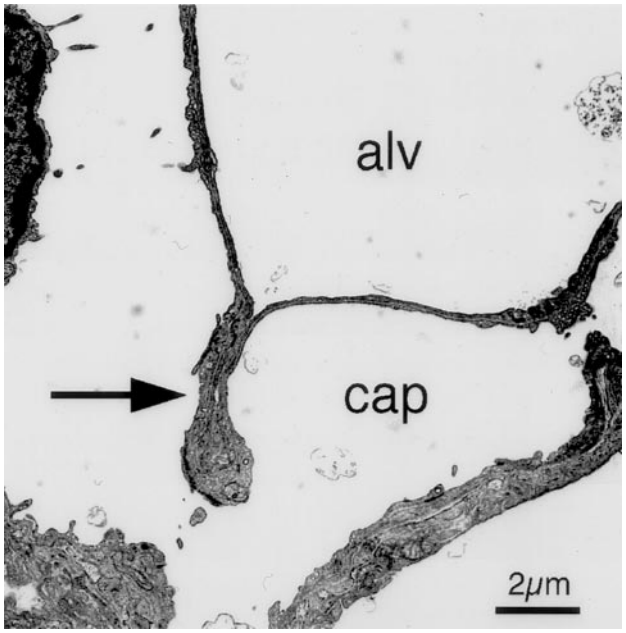

Fig. 4. Sample electron micrograph demonstrating folding (arrow) of tissue separating alveolar (alv) and capillary (cap) compartments at low lung volume. Septal folding would allow large changes in lung volume without significant changes in EBMSA and is one mechanism that may be responsible for small changes in EBMSA as the lung is deflated close to residual volume. An alternative mechanism is alveolar duct volume changes, which could occur independently of changes in alveolar volume and EBMSA. Because of volume cycling before fixation, septal folding was qualitatively rare.

(16). Contraction of fixed tissue could lead to erroneously high surface densities and an overestimation of epithelial surface area as shown in Fig. 3 (2). However, fractional changes in EBMSA (Fig. 5) would be unaffected by a systematic shrinkage error. We examined all lungs under light microscopy (Fig. 2) and found that,

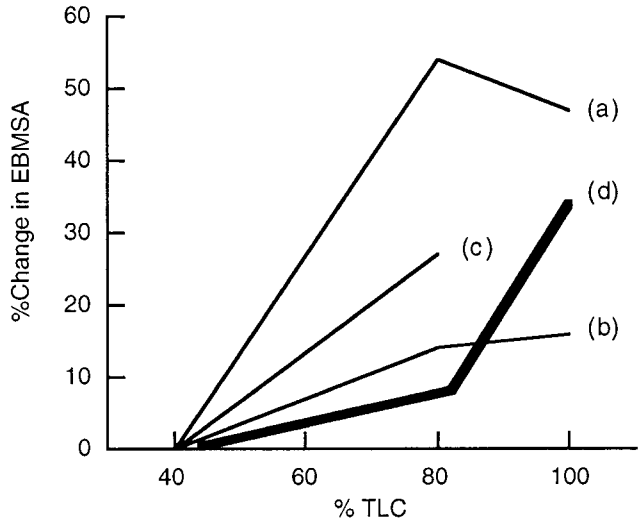

Fig. 5. Comparison of present study (*d*) with data of Bachofen et al. (*a-c*) (2). Percent increases in EBMSA were computed on inflation from collapse, relative to lungs fixed at 40% TLC on inflation (*a*); on deflation from TLC, relative to lungs fixed at 40% TLC on deflation (*b*); on reinflation from 40% TLC, relative to lungs fixed at 40% TLC on deflation (*c*); and on deflation from TLC, relative to lungs fixed at 40% TLC on deflation (*d*).

although the lungs fixed at high volumes exhibited some septal waviness, it was less than noted by Oldmixon et al. (16) in rabbit and dog lungs. These differences might be explained by the fact that, in rat lungs, the ratio of collagen to elastin is quite high (~8:1) in the alveolar walls (80–100 μm from the alveolar duct; Ref. 12). Fixation of collagen would tend to stabilize alveolar structure even in the absence of elastin fixation. No comparable collagen-to-elastin ratio is available for rabbits. In dog lungs, the collagen-to-elastin ratio is also highest in the alveolar walls (14), but the magnitude of the collagen-to-elastin ratio (~4:1) is much smaller than in the alveolar walls of rat lungs. Thus tissue deformation due to elastin contraction may be more prevalent in dog lungs fixed without ethanol dehydration. Although we cannot rule out the possibility that elastin contraction in our study resulted in small changes in alveolar geometry, the magnitude of our measured change in EBMSA is very similar to that measured in rabbit lungs fixed by using a technique that included ethanol dehydration (2). Thus we believe that tissue deformation due to either incomplete fixation or contraction of elastin was minimal in our study.

The second major difference between the Bachofen et al. (2) fixation protocol and that in the present study is the volume-cycling protocol that preceded lung fixation. Bachofen et al. fixed rabbit lungs on inflation from collapse (Ptp = 0.1–0.2 cmH_2O), on subsequent deflation from TLC, and on reinflation from 40% TLC. They reported that changes in EBMSA with lung volume depended greatly on where in the volume-cycling protocol the lungs were fixed. Furthermore, Oldmixon and Hoppin (15) examined in detail the relationship between septal folding and lung inflation history and concluded that alveolar septal folds may form de novo during experimental preparation, and significant folding may not be present in vivo. Specifically, they found the critical pressure for unfolding tissue was >16 cmH_2O, and the critical pressure for forming folds was <3 cmH_2O. There is some evidence that septal folds are absent in human lungs (21). We therefore cycled lung volume three times between TLC (above the critical unfolding pressure) and 8–10 cmH_2O (above the critical pressure for the formation of folds) before fixing on deflation to provide epithelial deformations representative of those in uniformly inflated lungs.

Despite the two differences in fixation protocol, the study of Bachofen et al. (2) represents the only previous measurement of EBMSA to which our data can be compared. To facilitate data comparison, we chose to express our results as %increases in EBMSA relative to 42% TLC (%$\Delta EBMSA_{42}$ in Table 2, Fig. 5, *d*). From the data of Bachofen et al., we computed the %increase in EBMSA relative to the EBMSA computed on either inflation or deflation at 40% TLC (Fig. 5, *a*-*c*). Note that *b* and *c* are based on a different baseline surface area than is *a*. It is clear that lungs fixed on inflation from collapse are not readily comparable to lungs fixed on deflation from TLC, either within the Bachofen study or in comparison with our data. The changes in EBMSA on inflation from collapse in the study by Bachofen et al. suggest that lung septal tissue stretches before reaching some critical unfolding pressure, hence the large changes in EBMSA at low lung volumes and the minimal change in EBMSA at high lung volume. This finding is contrary to our hypothesis that lung tissue unfolds at low lung volumes and stretches at high volumes. Supported by the findings of Oldmixon and Hoppin (15), we hypothesize that the state of the tissue at the beginning of the cycle is responsible for the dramatic difference in the data and that lungs fixed on deflation from high pressure are more representative of the in vivo condition.

The most comparable segment of the Bachofen et al. (2) protocol to the present study is the deflation from TLC (Fig. 5, *b*). Although we found a 34% change in EBMSA relative to 40% TLC, Bachofen et al. report a change of only 16%. It is difficult to explain the differences in these findings, except to attribute them to the distinctions in fixation and lung volume detailed previously. Although unlikely due to the reasons mentioned above, incomplete fixation might explain why our estimate of EBMSA at TLC could be high. Alternatively, the inconsistent results obtained by Bachofen et al. on each limb of the inflation-deflation cycle suggest that further volume cycling, as used in our study, is required to achieve uniformly inflated lungs with repeatable changes in EBMSA. The 27% change in EBMSA reported by Bachofen et al. on reinflation from 40 to 80% TLC (Fig. 5, *c*) would appear to support this second explanation. This 27% change in EBMSA is much greater than we find on deflation over the same lung volumes and is nearly as much as the total change in EBMSA we document on deflation from TLC to 40% TLC. The difficulty in comparing our data to those of Bachofen et al. underscores our motivation for examining lungs fixed after repetitive cycling.

A second piece of evidence that supports our EBMSA findings comes from morphological studies of collagen fibers in rat lungs. Mercer and Crapo (12) examined the collagen fibril geometry near alveolar septal edges in lungs fixed at 5 cmH_2O and found that fibrils could theoretically be extended 16 ± 3% before the wavelike structure of the fibrils would be straightened. Collagen fibers are thought to limit further extension of lung tissue once straightened (11). A change in length of 16% translates into a 32% change in surface area (see *Eq. 7* below), nearly identical to the 34% change in EBMSA we report on inflation from 3.8 to 25 cmH_2O. This agreement suggests that epithelial deformations parallel changes in extracellular fiber geometry.

The main purpose of this study was the derivation of a relationship between lung volume and EBMSA, which can be used as a guide for exposing alveolar epithelial cells to physiologically relevant deformations. Typically, alveolar epithelial cells are stretched on flexible substrates such as sponges or membranes. The deformation of cells grown on sponge substrates is not well characterized (9, 20). However, Scott et al. (19) and Wirtz and Dobbs (28) have examined the response of alveolar epithelial cells to more well-defined deformations on flexible membranes. Scott et al. studied fetal

cells by using a maximum of 10% membrane deformation at the periphery of the cell culture surface. The device provided a nonuniform deformation field, such that much of the culture surface was actually exposed to lower strains. By using *Eq. 7* (see below), a 10% deformation is roughly equivalent to a 20% change in surface area, well within our estimate of the physiological range for changes in EBMSA (Table 2). However, their strain protocol was selected to mimic deformations accompanying fetal breathing movements, which result in volume changes on the order of only 15% (8). Thus the imposed cell deformations may have been considerably larger than those experienced in vivo during fetal breathing movements.

Wirtz and Dobbs (28) developed a similar system to study type II alveolar epithelial cells isolated from mature rats. As in the study by Scott et al. (19), their device exposed cells to a nonuniform deformation field. They examined cell deformations ranging from 0 to 25% increases in cellular surface area and report that, above a 15% change in cellular surface area, phosphatidylcholine secretion was increased. This threshold deformation for phosphatidylcholine secretion would occur between 60 and 80% TLC (Table 2) and supports the authors' contention that periodic deep inflations may be important in stimulating surfactant secretion and maintaining lung compliance.

The measurement of EBMSA over a range of lung volumes reported here not only reveals the physiologically relevant range of cellular deformations but also yields important information regarding the contribution of alveolar walls to lung recoil. In lung mechanics, the connective tissue of the alveolar duct and surface tension at the air-liquid interface are often assumed to provide nearly all of the parenchymal elastic recoil on inflation (23, 27). Using the measurement of EBMSA obtained in this study, we can estimate the recoil pressure contributed by the basement membrane (Pmem), the primary load-bearing structure of the alveolar walls. From the principle of conservation of mechanical energy (23), the work done at the alveolar surface by Ptp during an incremental total lung volume change (dV_{tot}) is equal to the change in energy contributed by the membrane deformation plus the change in energy contributed by the change in tension at the air-liquid interface

$$Ptp * dV_{tot} = t * dS_{mem} + \gamma * dS_A \quad (3)$$

or

$$Ptp = t * \frac{dS_{mem}}{dV_{tot}} + \gamma * \frac{dS_A}{dV_{tot}} = Pmem + P\gamma \quad (4)$$

where t is the membrane tension, γ is surface tension, dS_{mem} is the incremental change in EBMSA, and dS_A is the incremental change in gas-exchange surface. Thus the contribution of membrane strain-energy to the recoil pressure is

$$Pmem = t * \frac{dS_{mem}}{dV_{tot}} \quad (5)$$

From continuum mechanics, the tension in a static elastic membrane is

$$t = E * h * \epsilon \quad (6)$$

where E is Young's modulus of the membrane material, h is the thickness of the membrane, and ϵ is the finite description of membrane deformation (4). We can use a value of 0.1 μm for h (26) and use measured values for E in the range of 2–20 MPa for epithelial basement membranes isolated from a variety of tissues (26). We can calculate finite strain from our measurement of change in surface area by using the relationship (4)

$$\epsilon = \frac{1}{2}(\%\Delta EBMSA_{24}/100\% \quad (7)$$

where $\%\Delta EBMSA_{24}$ is the percent increase in EBMSA relative to EBMSA measured at 24% TLC.

By using a second-order polynomial for the EBMSA-lung volume relationship, similar to that found for the EBMSA-%TLC relationship (Fig. 3), the following equation for the rat lung is obtained

$$EBMSA = S_{mem} = 2{,}344.9 - 53.3 * V_{tot} + 9.3 * V_{tot}^2 \quad (8)$$

where EBMSA is expressed in centimeters squared and V_{tot} in cubic centimeters. This yields

$$\frac{dS_{mem}}{dV} = -53.3 + 18.6 * V \quad (9)$$

Substituting *Eq. 9* into *Eq. 5*, Pmem at each fixation pressure can be computed. This calculation is critically dependent on the estimated stiffness of the alveolar epithelial basement membrane (E) and yields values for Pmem of 0.56–5.6 cmH_2O at TLC, depending on the stiffness used. Although Pmem increases as lung volume increases, the fraction of total recall pressure contributed by alveolar walls may or may not be significant, depending on the actual stiffness of the alveolar basement membrane, and highlights the need for a more definitive study of alveolar basement membrane mechanical properties. By using the larger estimate of Pmem, which incorporates the stiffness measured during large deformations in renal tubule basement membranes (26), stretching of the alveolar basement membrane is found to account for ~25% of total recoil pressure at TLC. This may explain the inability of previous models that neglect alveolar wall tension to accurately model lung behavior at volumes near TLC (23, 27).

In summary, the work presented in this communication provides an estimate of the epithelial deformations associated with quasi-static deflation over the vital capacity of isolated rat lungs. EBMSA was found to increase 5, 16, 12, and 40% relative to EBMSA at 24% TLC at lung volumes of 42, 60, 82, and 100% TLC, respectively. Extrapolation of these results to dynamically cycled human lungs requires great care. In addition, the difference in the order of unfolding and

stretching during deflation in the present study and that during inflation reported by Bachofen et al. (2) raises the possibility that dynamic cell deformations may be more complex than a simple reversible process. Nevertheless, this study contributes valuable information toward understanding the range of epithelial cell deformations associated with physiological changes in lung volume. These data are critical for relating deformation-induced lung cell behavior to in vivo lung volume changes and provide evidence that alveolar walls may make a measurable contribution to lung recoil at high volumes.

The authors thank Giuseppe Pietra for sharing his laboratory and invaluable experience; Lewis Johns for assistance with lung fixation and electron microscopy; Latressa Fulton and Jonathon Rogers for assistance with data analysis; and Ted Wilson for helpful discussions.

This work was supported by National Heart, Lung, and Blood Institute Grant HL-57204, National Science Foundation Grant BES-9702088, and the Whitaker Foundation. D. Tschumperlin was supported by a Whitaker Graduate Fellowship.

Address for reprint requests and other correspondence: S. Margulies, Dept. of Bioengineering, 240 S. 33rd St., Philadelphia, PA 19104–6392 (E-mail: margulies@seas.upenn.edu).

Received 1 July 1998; accepted in final form 11 February 1999.

REFERENCES

1. **Bachofen, H., A. Ammann, D. Wangensteen, and E. R. Weibel.** Perfusion fixation of lungs for structure-function analysis: credits and limitations. *J. Appl. Physiol.* 53: 528–533, 1982.
2. **Bachofen, H., S. Schürch, M. Urbinelli, and E. R. Weibel.** Relations among alveolar surface tension, surface area, volume, and recoil pressure. *J. Appl. Physiol.* 62: 1878–1887, 1987.
3. **Berg, J. T., Z. Fu, E. C. Breen, H.-C. Tran, O. Mathieu-Costello, and J. B. West.** High lung inflation increases mRNA levels of ECM components and growth factors in lung parenchyma. *J. Appl. Physiol.* 83: 120–128, 1997.
4. **Fung, Y. C.** *A First Course in Continuum Mechanics* (3rd ed.). Englewood Cliffs, NJ: Prentice-Hall, 1994, p. 112–124.
5. **Gil, J., H. Bachofen, P. Gehr, and E. R. Weibel.** Alveolar volume-surface area relation in air- and saline-filled lungs fixed by vascular perfusion. *J. Appl. Physiol.* 47: 990–1001, 1979.
6. **Gil, J., and E. R. Weibel.** Morphological study of pressure-volume hysteresis in rat lungs fixed by vascular perfusion. *Respir. Physiol.* 15: 190–213, 1972.
7. **Kim, K.-J., and E. D. Crandall.** Effects of lung inflation on alveolar epithelial solute and water transport properties. *J. Appl. Physiol.* 52: 1498–1505, 1982.
8. **Liggins, G. C., and J. A. Kitterman.** Development of the fetal lung. *Ciba. Found. Symp.* 86: 308–322, 1981.
9. **Liu, M., S. J. M. Skinner, J. Xu, R. N. N. Han, A. K. Tanswell, and M. Post.** Stimulation of fetal rat lung cell proliferation in vitro by mechanical stretch. *Am. J. Physiol.* 263 (*Lung Cell. Mol. Physiol.* 7): L376–L383, 1992.
10. **Massaro, G. D., and D. Massaro.** Morphologic evidence that large inflations of the lung stimulate secretion of surfactant. *Am. Rev. Respir. Dis.* 127: 235–236, 1983.
11. **Mead, J.** Mechanical properties of lungs. *Physiol. Rev.* 41: 281–328, 1961.
12. **Mercer, R. R., and J. D. Crapo.** Spatial distribution of collagen and elastin fibers in the lungs. *J. Appl. Physiol.* 69: 756–765, 1990.
13. **Mercer, R. R., J. M. Laco, and J. D. Crapo.** Three-dimensional reconstruction of alveoli in the rat lung for pressure-volume relationships. *J. Appl. Physiol.* 62: 1480–1487, 1987.
14. **Oldmixon, E. H., and F. G. Hoppin, Jr.** Distribution of elastin and collagen in canine lung alveolar parenchyma. *J. Appl. Physiol.* 67: 1941–1949, 1989.
15. **Oldmixon, E. H., and F. G. Hoppin, Jr.** Alveolar septal folding and lung inflation history. *J. Appl. Physiol.* 71: 2369–2379, 1991.
16. **Oldmixon, E. H., S. Suzuki, J. P. Butler, and F. G. Hoppin, Jr.** Perfusion dehydration fixes elastin and preserves lung air-space dimensions. *J. Appl. Physiol.* 58: 105–113, 1985.
17. **Rannels, D. E.** Role of physical forces in compensatory growth of the lung. *Am. J. Physiol.* 257 (*Lung Cell. Mol. Physiol.* 1): L179–L189, 1989.
18. **Scherle, W. A.** A simple method for volumetry of organs in quantitative stereology. *Mikroskopie* 26: 57–60, 1970.
19. **Scott, J. E., S.-Y. Yang, E. Stanik, and J. E. Anderson.** Influence of strain on [^{3}H]thymidine incorporation, surfactant-related phospholipid synthesis, and cAMP levels in fetal type II alveolar cells. *Am. J. Respir. Cell. Mol. Biol.* 8: 258–265, 1993.
20. **Skinner, S. J. M., C. E. Somervell, and D. M. Olson.** The effects of mechanical stretching on fetal rat lung cell prostacyclin production. *Prostaglandins* 43: 413–433, 1992.
21. **Sobin, S. S., Y. C. Fung, and H. M Tremer.** Collagen and elastin fibers in human pulmonary alveolar walls. *J. Appl. Physiol.* 64: 1659–1675, 1988.
22. **Stahl, W. R.** Scaling of respiratory variables in mammals. *J. Appl. Physiol.* 22: 453–460, 1967.
23. **Stamenovic, D.** Micromechanical foundations of pulmonary elasticity. *Physiol. Rev.* 70: 1117–1134, 1990.
24. **Weibel, E. R.** Morphometric estimation of pulmonary diffusion capacity. *Respir. Physiol.* 11: 54–75, 1970.
25. **Weibel, E. R.** *Stereological Methods: Practical Methods for Biologic Morphometry.* London: Academic, 1979, vol. 1, p. 31–37.
26. **Welling, L. W., M. T. Zupka, and D. J. Welling.** Mechanical properties of basement membrane. *News Physiol. Sci.* 10: 30–35, 1995.
27. **Wilson, T. A., and H. Bachofen.** A model for the mechanical structure of the alveolar duct. *J. Appl. Physiol.* 52: 1064–1070, 1982.
28. **Wirtz, H. R. W., and L. G. Dobbs.** Calcium mobilization and exocytosis after one mechanical stretch of lung epithelial cells. *Science* 250: 1266–1269, 1990.
29. **Zhang, S., V. Garbutt, and J. T. McBride.** Strain-induced growth of the immature lung. *J. Appl. Physiol.* 81: 1471–1476, 1996.